Evaluation of self-healing capability of a polycaprolactone interphase in epoxy/glass composites

L. Simonini [*], H. Mahmood, A. Dorigato, A. Pegoretti

Department of Industrial Engineering, University of Trento, Via Sommarive 9, 38123 Trento, Italy
National Interuniversity Consortium of Materials Science and Technology (INSTM), Via Giusti 9, 50121 Florence, Italy

ABSTRACT

Self-healing composites possess the ability to self-repair in response to damage, either autonomously (i.e., without human intervention), or when subjected to an external stimulus such as heat. This work was focused on the evaluation of the interfacial self-healing capability of glass fiber-reinforced epoxy composites in which polycaprolactone nanoparticles were deposited as a coating on the surface of the fibers. Polycaprolactone nanoparticles were synthesized following solvent displacement technique and deposited on the fibers (with and without the sizing agent) by electrophoretic deposition. Scanning electron microscopy revealed high-quality nanoparticles deposition, with good level of homogeneity and compactness. Epoxy microdroplets were cured on the fibers and microdebonding tests were performed to estimate the interfacial self-healing capability, calculated as the ratio of the interfacial shear stress measured before and after the thermal mending process. An interfacial adhesion recovery of about 50 % was obtained, thus indicating an interfacial self-healing capability induced by the polycaprolactone nanoparticles.

1. Introduction

Fiber-reinforced composites applied as structural materials are subjected to various loading conditions during their service life. The stresses resulting in the components may generate internal and/or external defects whose growth can compromise the structural integrity, ultimately leading to catastrophic failure. Defects detection, particularly those present internally, is often challenging and their repair is usually costly, making the replacement of the component more convenient rather than its repair. Therefore, in the last decades, self-healing materials have been widely investigated to overcome this limitation. Self-healing systems are a class of innovative materials that have the inherent ability to fully or partially recover their original mechanical properties after being damaged [1,2]. These systems are classified as intrinsic and extrinsic self-healing materials. Intrinsic systems can heal a crack through physical and chemical interactions at the molecular level. Those interactions can be stimulated by heat or by another physical stimulus (e.g., electrical voltage, magnetic field, etc.) [3,4]. On the other hand, the extrinsic systems include auxiliary components like microcapsules [5–7] and vascular networks [8–10] filled with a healing agent that is released when the crack propagates. The biggest advantage of the intrinsic

systems over the extrinsic ones is that the healing process is reversible i. e., multiple healing events can be carried out within the structure.

In the past years, both intrinsic and extrinsic self-healing systems have been widely investigated for polymer matrices of composite materials. Tesoro et al. [11] investigated reversible intrinsic epoxy matrices by the introduction of disulfide groups to obtain 90 % tensile strength recovery. Meure et al. [12] investigated the healing capability of poly [ethylene-co-(methacrylic acid)] (EMAA)/epoxy blends, highlighting the good compatibility between the two phases with an 85 % recovery of the fracture toughness upon thermal mending. Mahmood et al. [13,14] introduced cyclic olefin copolymer (COC) in an epoxy matrix, showing improvements in the healing efficiency up to 180 %. Patel et al. [15] studied the extrinsic self-healing behavior of glass fiber-reinforced epoxy composites containing microencapsulated dicyclopentadiene (DCPD) as healing agent.

However, the performance of composite materials does not depend only on the mechanical properties of their constituents (i.e., matrix and fibers), but it also relies on the physical properties of the interphase. A failure of the interphase prevents the matrix from transferring the load to the fibers, ultimately causing the composite to fail. To ensure the long-term reliability of structural components, it is therefore essential to

* Corresponding author at: Department of Industrial Engineering, University of Trento, Via Sommarive 9, 38123 Trento, Italy.
  E-mail address: laura.simonini@unitn.it (L. Simonini).

improve the mechanical stability of the interphase. In this region, several adhesion mechanisms can be established, like surface adsorption, molecular interdiffusion, electrostatic attraction, chemical bonding, and mechanical adhesion [16], which strongly affect the mechanical properties of the final composite. Chemical and physical treatments of the fibers surface can generally improve those interactions [17–21]. Recent works demonstrated that surface coating could be a powerful method for the mechanical optimization of the interphase while imparting specific functionalities to the final composite, like energy storage, healing, sensing, and strain monitoring capability [22–25]. The idea behind the present work is thus to create a multifunctional interphase by coating the fibers with polycaprolactone (PCL) deposited in form of nanoparticles through electrophoretic deposition (EPD) to impart good mechanical properties and self-healing capabilities. PCL is finding increasing scientific interest and attracting applications [26–28]. It is a thermoplastic biodegradable polyester with a low melting point of about 60 °C and glass transition temperature of about −60 °C. At room temperature, PCL is highly soluble in various solvents, like chloroform, benzene, toluene, dichloromethane, and acetone, and it has the property of being miscible with other polymers [29–31], including epoxy matrices (EP) [30,32–34]. In fact, one of the most recent applications of PCL is as a blending agent in epoxy systems for self-healing applications [35]. Karger-Kocsis [36] studied the thermally induced healing behavior of PCL/EP blends, reporting a healing efficiency of up to 80 % upon compact tension tests. Yao et al. [37] investigated the self-healing and shape memory capability of PCL/EP blends showing recovery of the tensile stress of 45 % compared to the neat EP samples. Recently, the use of PCL has been extended to self-healing interfaces in fiber-reinforced composites. Szebenyi et al. [38] investigated the positive results of interfacial engineered carbon fibers reinforced polymer (CFRP) composites where PCL is used as an interfacial 3D-printed interlayer material that increased the ductile pseudo-behavior of CFRPs.

This work aims to develop and characterize a nanostructured PCL-based multifunctional interphase in epoxy/glass fiber (GF) composites, able to provide self-healing capability at the interfacial level. PCL nanoparticles were synthesized by solvent-displacement method and subsequently deposited on the glass fibers' surface through an electrophoretic deposition method [39,40]. The obtained intrinsic self-healing interphase was characterized from a microstructural and mechanical point of view. Particular attention was devoted to the healing efficiency of this interphase, which was determined through microdebonding tests before and after the thermal mending process.

2. Experimental part

2.1. Materials

WINDSTRAND® glass fibers were provided by Owens Corning (Frankfurt, Germany) as rovings both silane-sized (density = 2.3 g/cm^3, bundle tex = 600, average fiber diameter = 18 μm, elastic modulus = 71 GPa) and unsized (density = 2.4 g/cm^3, bundle tex = 600, average fiber diameter = 18 μm, elastic modulus = 69 GPa). In this paper, sized fibers were designated as sGF, while the unsized ones were as uGF.

A bicomponent epoxy system constituted by an epoxy base (EC157.1) and an aminic hardener (W342) was provided by Elantas Italia S.r.l. (Collecchio, Italy) and it was used as the matrix for the composite systems analyzed. Both components were mixed at a weight ratio of 100:30 and cured for 8 h at room temperature, then for 40 h at 50 °C. This curing cycle was found to be optimal for this system after some preliminary trials. The cured epoxy resulted to have a glass transition temperature (T_g) equal to 84 °C, a thermal degradation temperature of 352 °C, an elastic modulus of 3.1 ± 0.2 GPa and tensile strength of 60.7 ± 15.3 MPa.

Facilan^{TM} Poly(ϵ-caprolactone) (PCL) was provided by 3D4makers B.V. (Haarlem, Netherlands) as a continuous filament (density = 1.1 g/

cm^3, average molecular weight (M_w) = 84500 g/mol) and it was used for the production of PCL nanoparticles to be deposited on glass fibers. Poly (vinyl alcohol) (PVA) (density = 1.2 g/cm^3, M_w = 50000 g/mol) and Polysorbate 80 (Tween® 80) (density = 1.1 g/cm^3, pH = 5.5–7.5) were provided by Sigma Aldrich (Missouri, USA) as a powder and a viscous liquid, respectively, and were used as stabilizers for the preparation of PCL nanoparticles [39]. All the materials were used as received.

2.2. Sample preparation

PCL nanoparticles were synthesized following the solvent displacement technique, described in detail by Badri et al. [39]. A part of the PCL filament was cut into short chips and dissolved in acetone under stirring for 30 min. The obtained solution (organic phase) was added dropwise at a constant injection rate in a well-stirred Milli-Q water solution containing dissolved PVA and Tween® 80 (aqueous phase). The resulting mixture was then poured into a rotating evaporation device (Rotavapor Buchi R-114) equipped with a water bath (Buchi B-480) and stirred under partial vacuum (600 mbar) at 30 °C till complete evaporation of the acetone was achieved. Table 1 shows the concentration of each component, the stirring speed applied for both the organic and the aqueous solution, and the injection rate of the organic phase in the water solution.

The obtained PCL water solution (0.5 mg/mL) was ultrasonicated for 15 min at room temperature by using a FALC (Shenzhen, China) ultrasonic bath to achieve better nanoparticle dispersion. Scanning electron microscopy observation (FESEM, Zeiss Supra 40, coating Pt/Pd (80:20)) of a single diluted drop of the prepared solution (dilution 1:10 in Milli-Q water) is reported in Fig. 1, together with a statistical distribution of the PCL particles size. The observation of the nanoparticles was conducted after the complete evaporation of the solvent that took 30 min at room temperature under vacuum. The particles presented a low level of agglomeration, indicating an efficient preparation method, and their average size was estimated equal to 65 ± 2 nm.

Then, the PCL water solution was diluted in Milli-Q water and three different PCL solution concentrations (0.01 wt%, 0.03 wt%, 0.05 wt%) were obtained. For each solution, the values of pH were calculated by using a PHD1 (PCE Instruments, Meschede, Germany) pH meter, while the values of zeta potential were calculated by using a Beckman Coulter DelsaNano AT Auto Tritator analyzer (Pasadena, USA), adding 0.1 M of HCl. The obtained values are reported in Table 2.

The analyzed solutions, regardless of the concentration, had a slightly acidic pH, strongly affected by the presence of the stabilizer Tween® 80. The Zeta potential values were negative and comprised between −11.4 and −16.0 mV, thus indicating potential particle instability, as reported in the literature [41]. The values of zeta potential were acceptable for this case study, but it could be helpful in the future to add larger quantities of the two stabilizers to try to improve the stability of the particles in the solution. Fiber coating was performed by electrophoretic deposition (EPD) [42,43]. A schematic view of the experimental setup is reported in Fig. 2a. Two copper plates were used as electrodes (i.e., anode and cathode) connected to a DC power supply (ISOTech IPS303DD). A copper window frame was used as glass fibers holder on which the GF bundles were glued on a bi-adhesive tape

Table 1
Parameters utilized for solvent displacement process.

	Parameters	Values
Organic phase	PCL concentration (mg/mL)	4
	Acetone (mL)	12.5
Water phase	Tween® 80 concentration (mg/mL)	21.2
	Milli-Q water concentration (mL)	100
	PVA concentration (mg/mL)	2.5
	Stirring speed (rpm)	600
	Injection rate (mL/min)	2.5
	Rotavapor rotating speed (rpm)	400
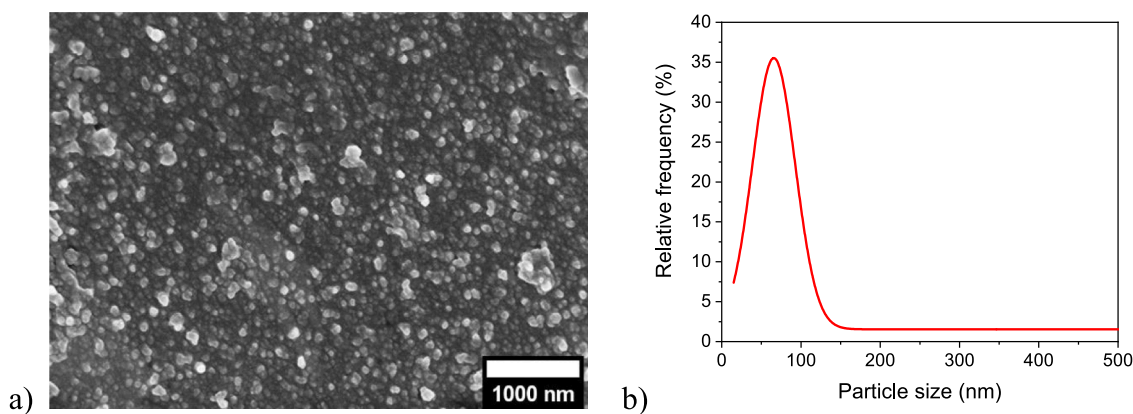
Fig. 1. (a) FESEM image of PCL nanoparticles, (b) statistical size distribution of PCL nanoparticles.

Table 2
Values of pH and zeta potential for PCL water solutions at different relative concentrations.

PCL concentration (wt.%)	pH	Zeta potential (mV)
0.01	5.3 ± 0.1	-16.0 ± 0.5
0.03	5.3 ± 0.1	-15.4 ± 1.7
0.05	5.4 ± 0.1	-11.4 ± 1.4

(Fig. 2b). The actual setup is shown in Fig. 2c. The measure of the zeta potential suggested that the nanoparticle flow was directed from the negative copper plate to the positive one. In order to perform the PCL deposition on both sides of the fiber bundles, the applied voltage was inverted after a defined deposition time.

A careful analysis of the deposition process was carried out to select the most suitable EPD parameters, in terms of geometrical configuration setup, time, and voltage, in order to obtain the highest PCL nanoparticles deposition quality as a function of the solution concentration. After several preliminary trials, the distance between the two electrodes and the distance between the positive electrode and the sample holder was taken as 20 mm and 10 mm respectively, while the deposition time and the voltage were varied. In particular, three voltages (5 V, 10 V, 30 V) and three different depositions times (30 s, 60 s, 120 s for each bundle side) were employed. Note that the position of the fibers in the bundle during the deposition process may affect the homogeneity of the deposition itself since the innermost fibers could be less coated than the outermost fibers. Therefore, the possibility of using bundles with low tex may be taken into account to ensure that the nanoparticles reach efficiently even the innermost fibers in the bundle. After being coated, the fibers were left to dry overnight at room temperature under vacuum. The identification of the prepared coated fibers is reported in Table 3.

Fig. 3 (a-d) shows an example of the visual appearance of the glass fibers attached to the copper holder before and after EPD. The PCL coating was not visible by the naked eye for both sGF and uGF. The unsized fibers resulted to be more difficult to be treated because the bundles tended to open and lose their orientation during the deposition process.

2.3. Experimental techniques

The morphological analysis of the uncoated and PCL coated fibers was performed by a Zeiss Supra 40 field-emission scanning electron microscope (FESEM), operating at an acceleration voltage of 3.5 kV. Prior to the analysis, the samples were coated with a Pt/Pd alloy (80:20) coating having a thickness of about 5 nm.

Thermogravimetric analysis (TGA) was carried out in order to evaluate the amount of PCL nanoparticles deposited on the surface of GF, by comparing the residual mass at the end of the thermal treatment

Table 3
List of prepared coated fibers.

Sample name	PCL solution concentration (wt.%)	ΔV(V)	Time(s)
sGF / uGF	–	–	–
Constant deposition time (t) = 60 s			
(s/u)GF_0.01_5_60	0.01	5	60
(s/u)GF_0.01_10_60	0.01	10	60
(s/u)GF_0.01_30_60	0.01	30	60
(s/u)GF_0.03_5_60	0.03	5	60
(s/u)GF_0.03_10_60	0.03	10	60
(s/u)GF_0.03_30_60	0.03	30	60
(s/u)GF_0.05_5_60	0.05	5	60
(s/u)GF_0.05_10_60	0.05	10	60
(s/u)GF_0.05_30_60	0.05	30	60
Constant applied voltage (ΔV) = 30 V			
(s/u)GF_0.03_30_30	0.03	30	30
(s/u)GF_0.03_30_60	0.03	30	60
(s/u)GF_0.03_30_120	0.03	30	120
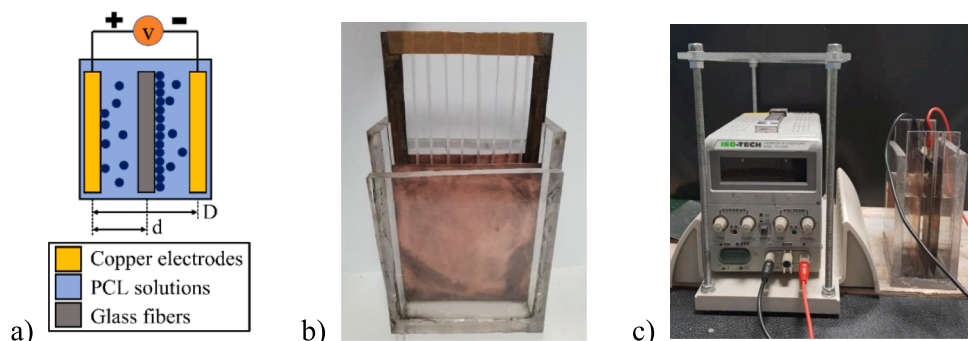
Fig. 2. Representative images of (a) EPD schematic setup, (b) glass fibers holder, (c) EPD actual setup.
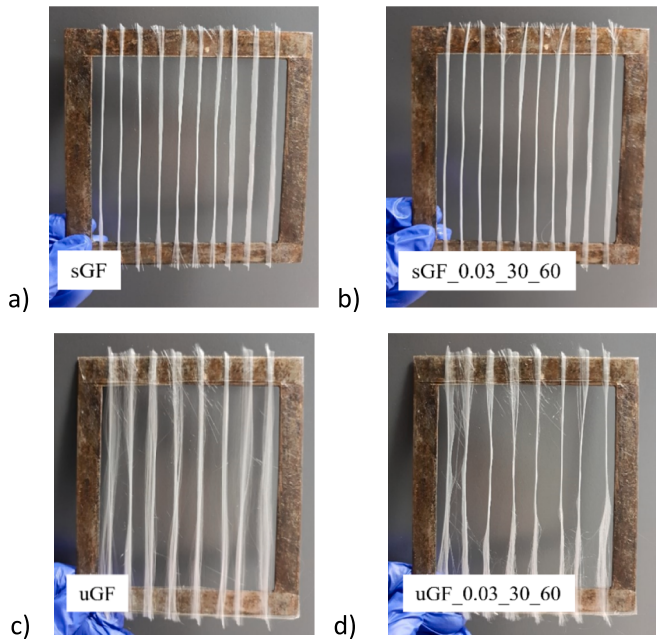
Fig. 3. Representative images of the GF bundles before and after the EPD process. (a) sGF, (b) sGF_0.03_30_60, (c) uGF, (d) uGF_0.03_30_60.

(m_{700}) of the coated fibers with respect to the uncoated ones. The measurements were performed by using a TA-IQ5000 IR (New Castle, USA) thermobalance under an airflow of 100 mL/min in a temperature interval from 35 °C to 700 °C and at a heating rate of 10 °C/min.

Mechanical analysis was performed to investigate the interfacial self-healing capability provided by the PCL coating in epoxy/GF composites. Microdebonding tests were performed by gluing a single GF fiber on paper tabs with a gauge length equal to 15 mm. One single microdroplet of uncured epoxy resin (volume of about 0.001 mm^3) was deposited on each specimen by using a micropipette. In Fig. 4, representative images of a sample prepared for microdebonding tests are shown, analyzed by using a Nikon SMZ25 microscope, equipped with a Nikon DS-Fi2 digital camera.

Samples were left at room temperature for 8 h and then cured at 50 °C for 40 h in the oven. At least five specimens for each sample were tested. The microdebonding tests were conducted at a crosshead speed of 0.75 mm/min using an Instron 4502 (Norwood, USA) universal testing machine equipped with a 2.5 N load cell, as already described in previous articles [22,44–46]. The ratio between the maximum load (F_{max}) at which the matrix/fiber interphase failed and their contact area

resulted in the interfacial shear strength (IFSS), as reported in Equation (1):

$$IFSS = \frac{F_{max}}{\pi d L} \tag{1}$$

The contact area was calculated by measuring the diameter of the single fiber (d) and the bonding length (L), corresponding to the length of the epoxy drop in contact with the fiber, by using a Nikon SMZ25 microscope, equipped with a Nikon DS-Fi2 digital camera. The average debonding length was measured equal to 375 ± 25 μm. In the same way, it was possible to evaluate the interfacial adhesion values between the matrix and the PCL coated fibers (IFSS$_{PCL}$) considering F_{max} as the maximum load at which the matrix/(PCL coated) fiber interphase failed and d as the diameter of the single PCL coated fiber.

The post-damage frictional response of uncoated and PCL-coated fibers was investigated by control tests consisting of post-debonding run at room temperature after a 60-minute waiting time. In this sense, the interfacial adhesion values for post-debonding behavior were evaluated as IFSS$_{CONTROL}$, considering F_{max} as the post-damage frictional load and d as the diameter of the single uncoated or PCL coated fiber.

The thermal healing of the microdebonded specimens was performed by heating them in an oven at 80 °C for 1 h, as previously indicated by Invernizzi et. al. [47]. It is important to notice that this temperature is above the melting point of PCL (60 °C) and below the glass transition temperature (T_g) of the epoxy resin (84 °C), thus to maximize the healing efficiency [36,48]. After being healed, the samples were re-tested following the same procedure previously described. The gross healing efficiency (HE$_%$) was calculated as the ratio between the interfacial shear strength values after (IFSS$_{PCL\_H}$) and before (IFSS$_{PCL}$) the healing process, as reported in Equation (2).

$$HE_% = \frac{IFSS_{PCL\_H}}{IFSS_{PCL}} \times 100 \tag{2}$$

Since the operating temperature for the healing is in the proximity of the T_g of the epoxy resin, a residual curing step of the matrix might occur, which could contribute to the healing of the interphase. Therefore, a thermal treatment corresponding to the healing process was performed on the uncoated fibers on which a single epoxy drop was deposited in order to estimate the contribution of the epoxy residual curing on the interfacial healing. The values of mechanical adhesion after the heating treatment (IFSS$_H$) in these samples were calculated as reported in Equation (1). These values were multiplied by a factor k (Equation (3)), defined as the ratio between the adhesion values on the PCL coated fibers (IFSS$_{PCL}$) and the adhesion values on the uncoated fibers (IFSS). This is to correlate the effect of epoxy resin adhesion measured on the uncoated fibers as it would be measured on the PCL coated fibers. The normalized terms were then subtracted from the adhesion values of the functionalized healed interphase (IFSS$_{PCL\_H}$) and divided by IFSS$_{PCL}$, as reported in Equation (4). The result is the net healing efficiency (HE$_{NET%}$) and it indicates the contribution on the self-healing efficiency provided by the PCL coating only.

$$k = \frac{IFSS_{PCL}}{IFSS} \tag{3}$$

$$HE_{NET%} = \frac{IFSS_{PCL\_H} - (IFSS_H \times k)}{IFSS_{PCL}} \tag{4}$$

From Equation (2) and Equation (4), it is possible to calculate the contribution of the epoxy residual curing (EP$_%$), that is the difference between HE$_%$ and HE$_{NET%}$ values, as reported in Equation (5).

$$EP_% = HE_% - HE_{NET%} \tag{5}$$
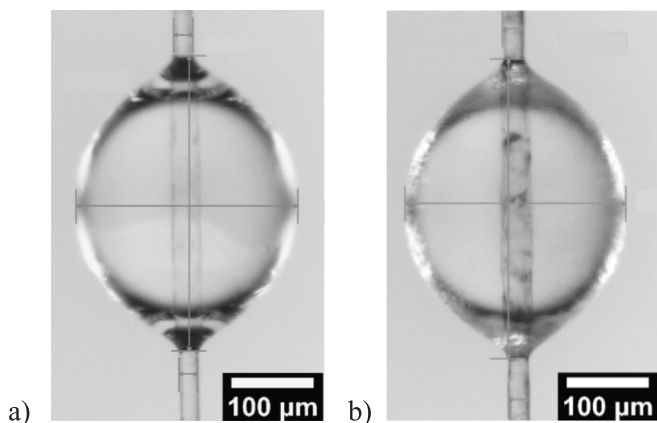
Fig. 4. Representative images of a sample prepared for microdebonding tests. In particular, (a) sGF, (b) sGF_0.03_30_60.

3. Results and discussion

3.1. Morphological characterization of PCL coated glass fibers

Fig. 5 compares the SEM images of the fibers coated by EPD technique and the uncoated ones. Both sized (sGF) and unsized (uGF) fibers are considered.

Regardless of the presence of the PCL coating, increasing both the solution concentration and the applied voltage, the deposition of PCL nanoparticles on GF increases. A consistent and homogeneous deposition can be observed by setting a potential of 30 V and a solution concentration of 0.03 wt%. After this preliminary analysis, these two parameters were kept constant and the time of deposition was changed (30 s, 60 s and 120 s for each bundle's side). The effect of the deposition time on the morphology of the coated fibers (both sGF and uGF) can be observed in Fig. 6.

It can be noticed that the longer the deposition time, the worse the homogeneity of the PCL coating. A compact and homogeneous coating can be obtained by selecting a deposition time equal to 60 s for each bundles side (total deposition time = 120 s). It can be also observed that this value of deposition time prevents the oxidation of the copper electrodes which begins after 150 s of deposition (at $\Delta V = 30$ V). This oxidation also leads to a change of the solution color that passes from matt white to green, because of the release of copper ions. This phenomenon is more evident by increasing the deposition duration.

The amount of PCL deposition as a function of the deposition time was evaluated by a TGA analysis. In Fig. 7(a-b) representative TGA thermograms for both sized and unsized GFs are reported.

In Table 4, the values of residual mass at 700 °C for each sample are reported.

A slight mass loss is measured for all the PCL coated fibers, which corresponds to the loss of the PCL coating, the silane coating (for the sized fibers) and other superficial impurities. sGF_0.03_30_60 and uGF_0.03_30_60 show the highest mass loss at the end of the thermal treatment (6.6 % and 7.9 % respectively), highlighting the fact that after 60 s of deposition time (for each side of the bundles) an optimum of

deposition was reached. For longer EPD treatments (sGF_0.03_30_120 and uGF_0.03_30_120 sample) and a lower mass loss was obtained. This could be due to the fact that the longer the deposition time, the more nanoparticles are deposited on the fibers, hence forming a multilayer coating. The last layers may not be as well adherent to the fibers' surface as the first ones, causing their detachment.

Therefore, based on the FESEM images and TGA analysis, a deposition time of 60 s (for both sides), a solution concentration of 0.03 wt% and an applied voltage of 30 V were selected as the best parameters to coat the glass fibers and to evaluate the interfacial self-healing capability of EP/GF composites through microdebonding tests.

3.2. Evaluation of the self-healing capability of the PCL interphase

In Fig. 8(a-b), the representative load–displacement curves obtained from microdebonding tests on the uncoated and PCL coated glass fibers are reported and compared with the curves relative to the healed and control samples (denoted by terms "H" and "control" in the sample code, respectively).

Looking at Fig. 8a, the epoxy drop on uncoated sGF specimen debonds at an appreciable load of 0.50 N, then slides on the fiber with a frictional resistance of 0.15 N. This frictional plateau is important since confirms the debonding of the epoxy drop. After the thermal mending procedure, the same epoxy drop debonds at a force of approximately 0.20 N, which is lower than the debonding force for the virgin test. Partial recovery of the virgin debonding force is attributed to thermal mending of epoxy with the fiber on account of additional cross-linking via residual functionality within the epoxy matrix. In the case of sGF_0.03_30_60, the epoxy drop debonds at load even higher than uncoated sGF sample (approx. 0.58 N) which indicates a higher adhesional interfacial bonding between epoxy and the fiber. This is another positive aspect verified by the coating of PCL nanoparticles on the fibers. After healing, the load recovered is 0.32 N, which is higher compared to healed uncoated sGF fibers. The higher load recovery is clearly a verification of the healing capability at interfacial level by the PCL healing agent.
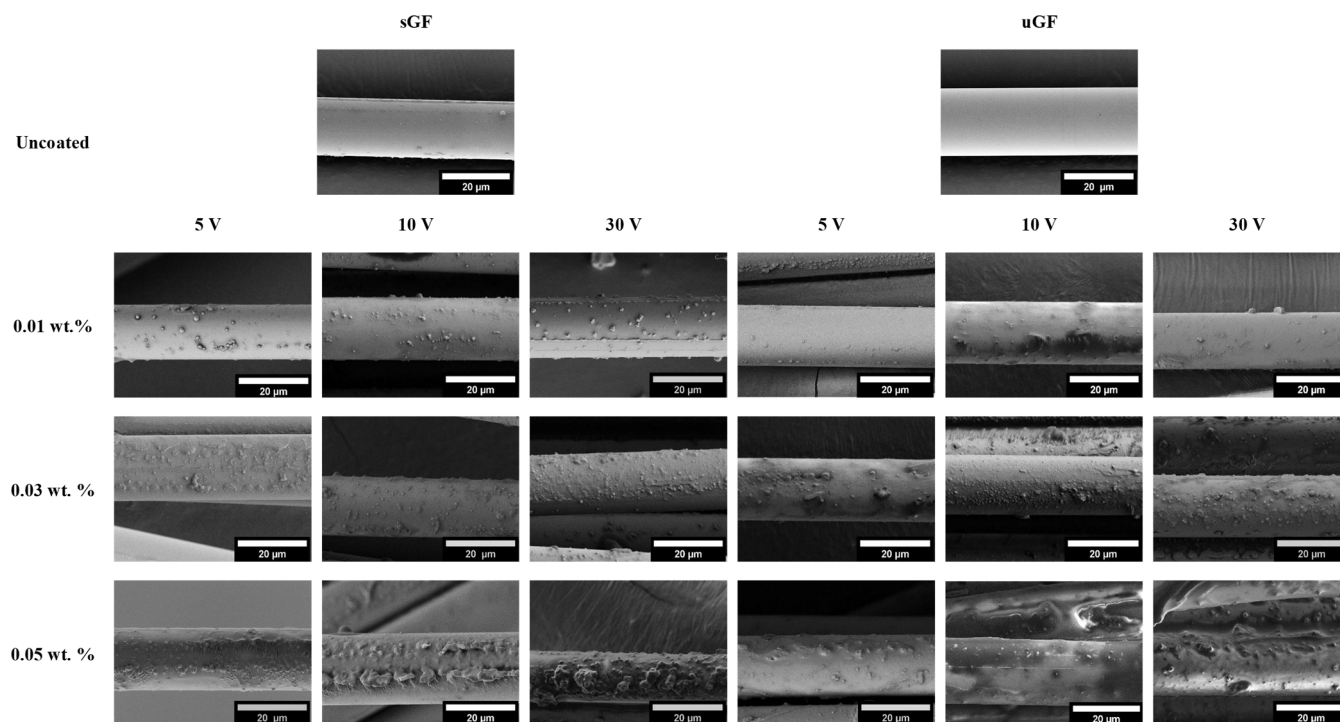
Fig. 5. SEM images of uncoated fibers and PCL coated fibers. The PCL solution concentration and the applied voltage were varied (5–30 V), while the deposition time was fixed (60 s for each side of the bundle).

30 s   **60 s**   **120 s**
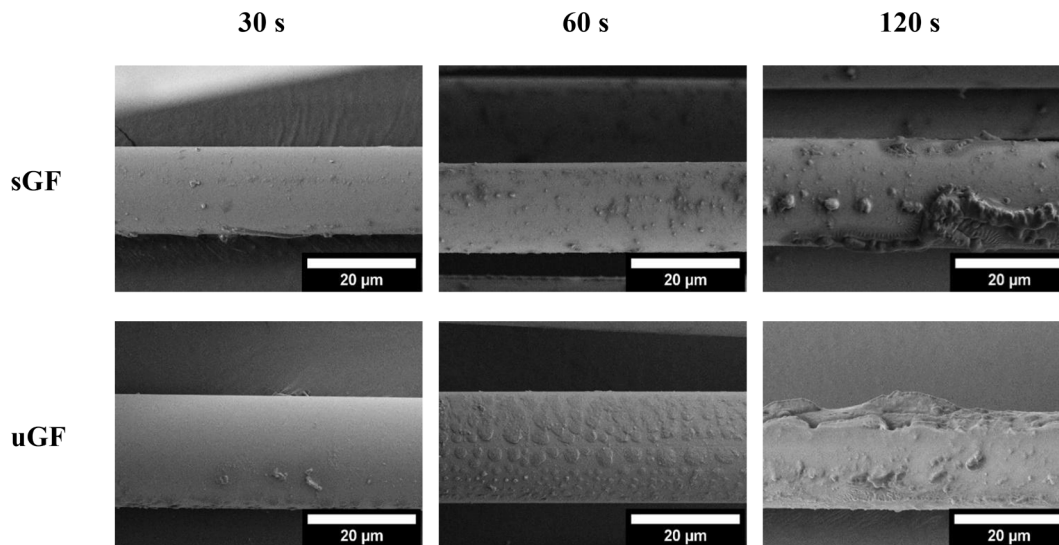
Fig. 6. SEM images of PCL coated fibers. The solution concentration (0.03 wt%) and the applied voltage (30 V) are fixed, while the time of deposition varies from 30 to 120 s for each side of the bundles.
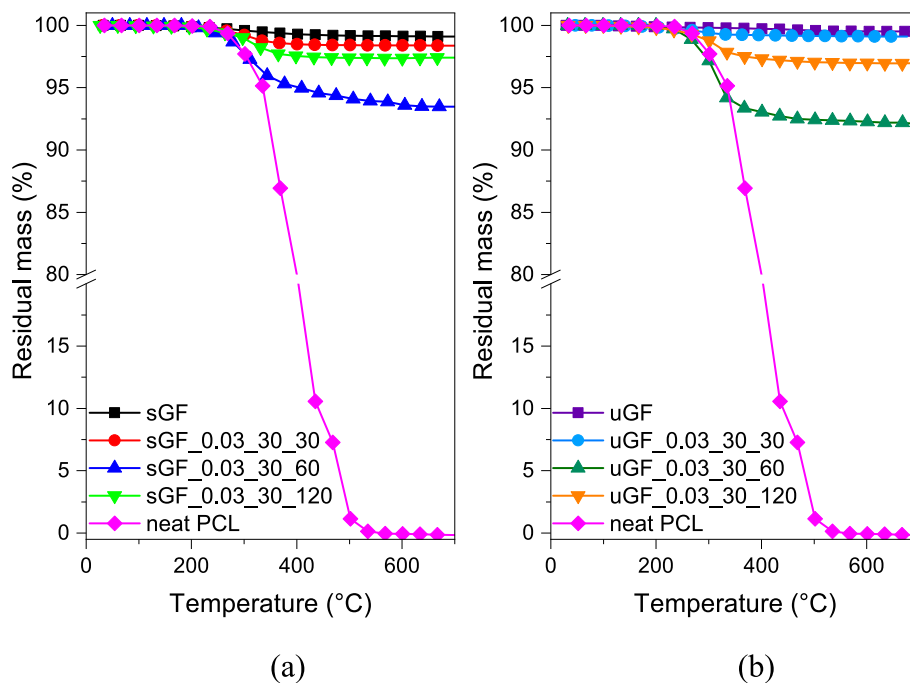
Fig. 7. TGA thermograms of neat PCL, uncoated and PCL coated fibers as a function of the deposition time, (a) sGF fibers, (b) uGF fibers.

Table 4
Values of residual mass at 700 °C(m_{700}) from TGA tests on the prepared fibers.

Samples	m_{700} (%)	Samples	m_{700} (%)
sGF	99.1	uGF	99.5
sGF_0.03_30_30	98.4	uGF_0.03_30_30	99.1
sGF_0.03_30_60	93.5	uGF_0.03_30_60	92.1
sGF_0.03_30_120	97.4	uGF_0.03_30_120	97.0

Even after the confirmation of this damage recovery, it was worthwhile to confirm any healing mechanism that might be acting other than the thermal mending procedure employed. Hence the control tests of virgin specimens were also performed by post-debonding run at room temperature after a 60-minute waiting time. From Fig. 8b, it can be observed that the control samples only exhibit the frictional force after

60 min from initial testing. Particularly, the control specimens of sGF-type of fibers show an initial peak of load corresponding to the static friction to move the microdrop. The same is true for fibers coated with PCL nanoparticles i.e., sGF_0.03_30_60. Hence the absence of any load higher than the frictional plateau confirms the absence of healing other than thermal mending performed on the samples.

On the other hand (Fig. 8c), in the case of samples involving uGF, a similar behavior of debonding/healing is found. The only difference is with the debonding force of virgin specimens involving PCL coating, which is similar to the uncoated uGF samples. Overall, also for uGF-type of fibers, the healing capability of PCL as an interphase between epoxy and GF is confirmed by microdebonding tests. The verification of the healing mechanism was also carried out by the post-debonding waiting time of 60 min. It can be seen from Fig. 8d that the control samples of uGF-type fibers only show a frictional plateau with loads corresponding

a)

b)

c)

d)
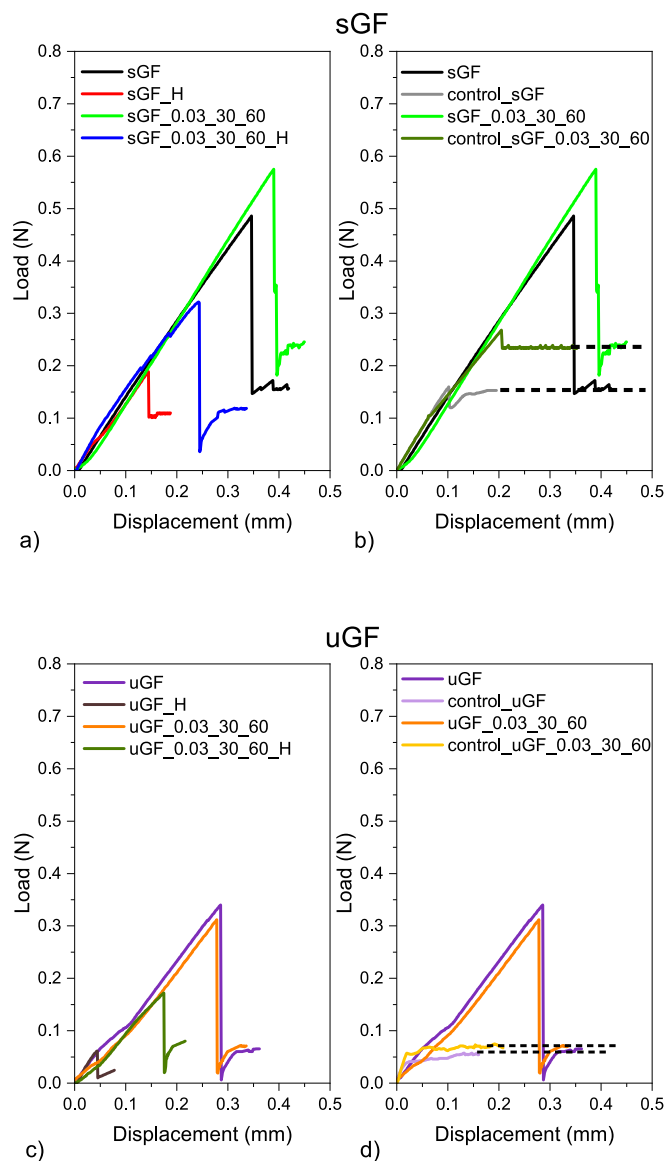
Fig. 8. Comparison of load-displacement curves from microdebonding tests on the uncoated fibers, PCL coated fibers and the corresponding healed and control samples for (a, b) sGF and (c, d) uGF.

to the frictional plateau of the original virgin specimens. More importantly, there is no peak load related to the static friction of the microdrop on the fiber. It may be concluded that the presence of the silane coating implies greater compatibility with the matrix thus requiring a force to overcome the static friction at the interphase.

Carefully analyzing the frictional plateau of the control samples and

healed samples, it is also observed that for control samples the resulting frictional loads are higher compared to the healed samples. This behavior can be explained by the different morphology of the coating before and after the thermal treatment. An example of FESEM images of the resulting morphology of the PCL coating is reported in Fig. 9. As expected, PCL melted during healing, therefore, passing from a rougher morphology to a film-like one, implying a lower frictional force during debonding.

A comparison of the obtained IFSS values is reported in Fig. 10a. These values were used for the calculation of the healing efficiency, according to the expressions reported in Equations (2)-(5) (see Fig. 10b).

a)

b)
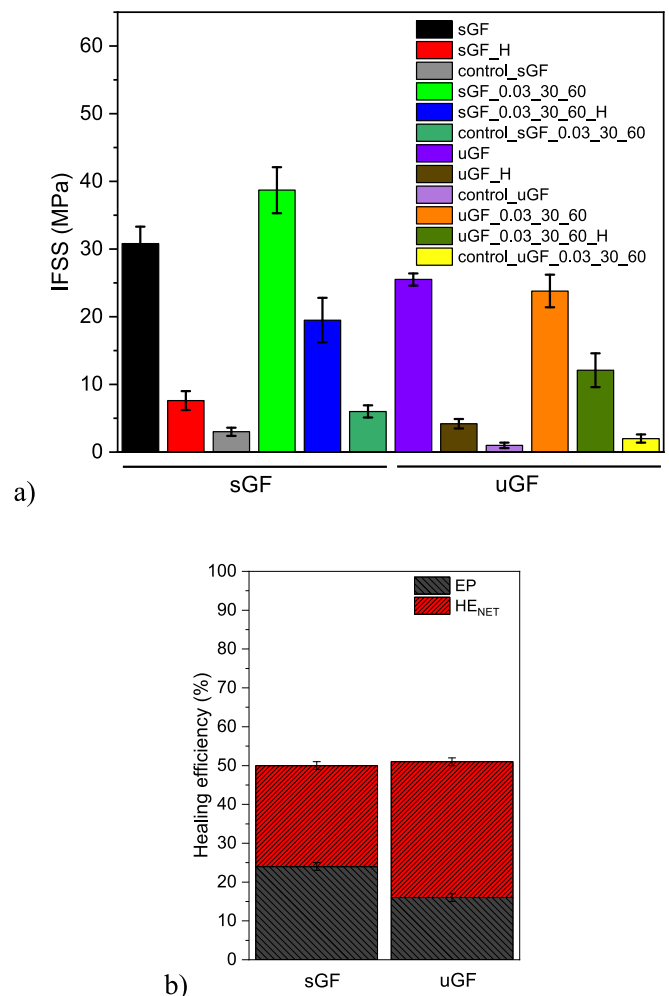
Fig. 10. Results of microdebonding tests on uncoated fibers, PCL coated fibers and the corresponding healed and control samples. (a) IFSS values, (b) healing efficiency values (see Equations (2)-(5)).
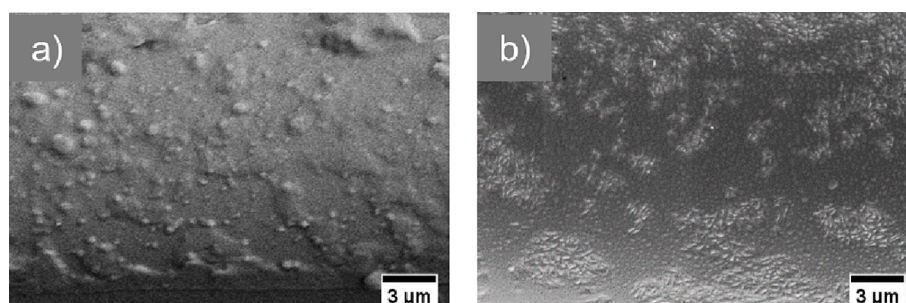
Fig. 9. FESEM morphology of PCL coating on fibers, a) before healing and b) after healing.

For each sample, the mean and the standard deviation values are reported and calculated from ten tested specimens.

From Fig. 10a, it is possible to see that the interfacial adhesion value of sGF is higher than uGF, due to the presence of the sizing agent. The IFSS values of the corresponding PCL coated samples (sGF_0.03_30_60 and uGF_0.03_30_60, respectively) demonstrate that the presence of the PCL interphase provides a positive effect in terms of interfacial shear strength in the case of sGF (+26 %), while no significant modifications can be noticed for uGF. This indicates that the PCL interphase has a positive interaction with the surface sizing applied on GFs. As it could be expected, the IFSS values of sGF_H and uGF_H are rather low, indicating a limited interfacial strength recovery without the PCL interphase. Once PCL nanoparticles are deposited on the surface of GF (with or without the sizing agent), a substantial recovery of the IFSS can be observed. The calculation of the healing efficiency (see Fig. 10b) demonstrates that the PCL interphase provides an IFSS recovery of 50 % upon thermal healing for sGF, and 51 % for uGF. In this case, the presence of the sizing agent does not seem to substantially influence the overall healing capability of these systems.

On the other hand, also the contribution played by the residual curing of the epoxy resin during the healing process should be considered. sGF_H and uGF_H samples showed respectively 24.7 % and 16.5 % recovery of the adhesion properties than neat fibers, indicating that also the residual curing of the matrix contributed to the interfacial healing process (Fig. 10a). This contribution is stronger in the case of sGF_H than uGF_H, probably because the sizing agent can physically (or chemically) interact with the epoxy resin. However, further studies should be performed in the future to have a better explanation of this result. The evaluation of the net healing efficiency ($HE_{NET\%}$) allows estimating the effective contribution given by the PCL interphase. $HE_{NET\%}$ values are respectively 52 % and 68 % of the overall healing efficiency for sGF and uGF coated fibers, demonstrating thus the potential of the PCL coating as healable interphase in epoxy/glass fibers composites.

Further efforts are required to enhance the interfacial healing efficiency of PCL coated glass/epoxy composites, by adding suitable compatibilizers to the PCL nanoparticles dispersed in solution to improve the chemical interactions between the healing agent and the epoxy matrix, therefore strengthening the potential of PCL as a healable interphase. Also, the repeatability of the interfacial healing process could be evaluated, by performing microdebonding tests on the samples after multiple thermal treatments.

4. Conclusions

For the first time, PCL nanoparticles were used as a self-healing interphase between an epoxy matrix and glass fibers. The nanoparticles were prepared by a solvent displacement technique, and they were dispersed in water at different concentrations. PCL nanoparticle deposition on the glass fibers surface was performed by EPD (both sized and unsized fibers were considered). The morphological analysis showed that the quality of deposition was strongly affected by the process parameters (i.e., deposition time, applied voltage, PCL solution concentration). A homogeneous PCL coating on glass fibers was obtained by a deposition performed at 30 V for 60 s on each side of the fibers, by using a PCL solution concentration of 0.03 wt% PCL. Microdebonding tests were performed by using both uncoated and coated fibers and a cured epoxy droplet, and the tested specimens were then thermally treated at 80 °C for 1 h to evaluate the healing efficiency of the PCL coating, through the evaluation of the IFSS values. It was observed that, regardless of the presence of the sizing agent on GF surface, an overall IFSS recovery of about 50 % was obtained upon the healing process, indicating that PCL nanoparticles coating on GFs could be an interesting option for the interfacial thermal mending of epoxy/glass composites. Also, the residual curing of the epoxy matrix during the healing process contributes to the recovery of the interfacial strength in these microcomposites.

CRediT authorship contribution statement

L. Simonini: Conceptualization, Investigation, Methodology, Data curation, Writing – original draft, Visualization, Validation. **H. Mahmood:** Conceptualization, Methodology, Visualization, Validation. **A. Dorigato:** Conceptualization, Funding acquisition, Supervision, Visualization, Validation. **A. Pegoretti:** Conceptualization, Funding acquisition, Supervision, Visualization, Validation.

Declaration of Competing Interest

The authors declare that they have no known competing financial interests or personal relationships that could have appeared to influence the work reported in this paper.

Data availability

Data will be made available on request.

References

[1] Cohades A, Branfoot C, Rae S, Bond I, Michaud V. Progress in Self-Healing Fiber-Reinforced Polymer Composites. Adv Mater Interfaces 2018;5(17).

[2] Blaiszik BJ, Kramer SLB, Olugebefola SC, Moore JS, Sottos NR, White SR. Self-Healing Polymers and Composites. Annu Rev Mat Res 2010;40:179–211.

[3] Hu Z, Zhang D, Lu F, Yuan W, Xu X, Zhang Q, et al. Multistimuli-Responsive Intrinsic Self-Healing Epoxy Resin Constructed by Host-Guest Interactions. Macromolecules 2018;51(14):5294–303.

[4] Guimard NK, Oehlenschlaeger KK, Zhou J, Hilf S, Schmidt FG, Barner-Kowollik C. Current Trends in the Field of Self-Healing Materials. Macromol Chem Phys 2012; 213(2):131–43.

[5] Kosarli M, Bekas DG, Tsirka K, Baltzis D, Vaimakis-Tsogkas DT, Orfanidis S, et al. Microcapsule-based self-healing materials: Healing efficiency and toughness reduction vs. capsule size. Compos B Eng 2019;171:78–86.

[6] Hia IL, Chan E-S, Chai S-P, Pasbakhsh P. A novel repeated self-healing epoxy composite with alginate multicore microcapsules. J Mater Chem A 2018;6(18): 8470–8.

[7] Wang Y, Li Y, Zhang Z, Zhao H, Zhang Y. Repair Performance of Self-Healing Microcapsule/Epoxy Resin Insulating Composite to Physical Damage. Appl Sci 2019;9(19):4098.

[8] Malekkhouyan R, Neisiany RE, Khorasani SN, Das O, Berto F, Ramakrishna S. The influence of size and healing content on the performance of extrinsic self-healing coatings. J Appl Polym Sci 2020;138(10):49964.

[9] Postiglione G, Alberini M, Leigh S, Levi M, Turri S. Effect of 3D-Printed Microvascular Network Design on the Self-Healing Behavior of Cross-Linked Polymers. ACS Appl Mater Interfaces 2017;9(16):14371–8.

[10] Patrick JF, Hart KR, Krull BP, Diesendruck CE, Moore JS, White SR, et al. Continuous self-healing life cycle in vascularized structural composites. Adv Mater 2014;26(25):4302–8.

[11] Tesoro G, Sastri V. Reversible crosslinking in epoxy resins. I. Feasibility studies. J Appl Polym Sci 1990;39(7):1425–37.

[12] Meure S, Wu DY, Furman S. Polyethylene-co-methacrylic acid healing agents for mendable epoxy resins. Acta Mater 2009;57(14):4312–20.

[13] Zovi RC, Mahmood H, Dorigato A, Fredi G, Pegoretti A. Cyclic Olefin Copolymer Interleaves for Thermally Mendable Carbon/Epoxy Laminates. Molecules 2020;25 (22):5347.

[14] Mahmood H, Dorigato A, Pegoretti A. Healable Carbon Fiber-Reinforced Epoxy/ Cyclic Olefin Copolymer Composites. Materials 2020;13(9):2165.

[15] Patel AJ, Sottos NR, Wetzel ED, White S. Autonomic healing of low-velocity impact damage in fiber-reinforced composites. Compos A Appl Sci Manuf 2010;41(3): 360–8.

[16] Da Silva L, Marques E, Campilho R. Design Rules and Methods to Improve Joint Strength. Handbook of Adhesion Technology; 2018. p. 773–810.

[17] Chen J, Zhu Y, Ni Q, Fu Y, Fu X. Surface modification and characterization of aramid fibers with hybrid coating. Appl Surf Sci 2014;321:103–8.

[18] Mohit H, Selvan V. AM. A comprehensive review on surface modification, structure interface and bonding mechanism of plant cellulose fiber reinforced polymer based composites. Compos Interfaces 2018;25(5–7):629–67.

[19] Raphael N, Namratha K, Chandrashekar BN, Sadasivuni KK, Ponnamma D, Smitha AS, et al. Surface modification and grafting of carbon fibers: A route to better interface. Prog Cryst Growth Charact Mater 2018;64(3):75–101.

[20] Vedrtnam A, Sharma SP. Study on the performance of different nano-species used for surface modification of carbon fiber for interface strengthening. Compos A Appl Sci Manuf 2019;125:105509.

[21] Zhang W, Deng X, Sui G, Yang X. Improving interfacial and mechanical properties of carbon nanotube-sized carbon fiber/epoxy composites. Carbon 2019;145: 629–39.

[22] Mahmood H, Simonini L, Dorigato A, Pegoretti A. Graphene Deposition on Glass Fibers by Triboelectrification. Appl Sci 2021;11(7):3123.

[23] Qi H, Liu J, Mäder E. Smart Cellulose Fibers Coated with Carbon Nanotube Networks. Fibers 2014;2(4):295–307.

[24] Fredi G, Dorigato A, Fambri L, Pegoretti A. Multifunctional epoxy/carbon fiber laminates for thermal energy storage and release. Compos Sci Technol 2018;158: 101–11.

[25] Sorze A, Valentini F, Dorigato A, Pegoretti A. Salt leaching as a green method for the production of polyethylene foams for thermal energy storage applications. Polym Eng Sci 2022;62(5):1650–63.

[26] Malikmammadov E, Tanir TE, Kiziltay A, Hasirci V, Hasirci N. PCL and PCL-based materials in biomedical applications. J Biomater Sci Polym Ed 2018;29(7–9): 863–93.

[27] Cabedo L, Luis Feijoo J, Pilar Villanueva M, Lagarón JM, Giménez E. Optimization of biodegradable nanocomposites based on a PLA/PCL blends for food packaging applications. Macromolecular Symposia: Wiley Online Library; 2006. p. 191-7.

[28] Mohamed RM, Yusoh K. A review on the recent research of polycaprolactone (PCL). Advanced Materials Research: Trans Tech Publ; 2016. p. 249-55.

[29] De Juana R, Cortazar MJM. Study of the melting and crystallization behavior of binary poly (. epsilon.-caprolactone)/poly (hydroxy ether of bisphenol A) blends. Macromolecules 1993;26(5):1170–6.

[30] Barone L, Carciotto S, Cicala G, Recca Science. A. Thermomechanical properties of epoxy/poly (ε-caprolactone) blends. Polym Eng Sci 2006;46(11):1576–82.

[31] Fabbri P, Cannillo V, Sola A, Dorigato A, Chiellini F. Highly porous polycaprolactone-45S5 Bioglass® scaffolds for bone tissue engineering. Compos Sci Technol 2010;70(13):1869–78.

[32] Yeh JT, Wu CJ, Tsou CH, Chai WL, Chow JD, Huang CY, et al. Study on the crystallization, miscibility, morphology, properties of poly (lactic acid)/poly (ε-caprolactone) blends. Polym-Plast Technol Eng 2009;48(6):571–8.

[33] Ferri JM, Fenollar O, Jorda Vilaplana A, García-Sanoguera D, Balart R. Effect of miscibility on mechanical and thermal properties of poly (lactic acid)/ polycaprolactone blends. Polym Int 2016;65(4):453–63.

[34] Zheng S, Lü H, Chen C, Nie K, Guo Q. Epoxy resin/poly (ethylene oxide)(PEO) and poly (ε-caprolactone)(PCL) blends cured with 1, 3, 5-trihydroxybenzene: miscibility and intermolecular interactions. Colloid Polym Sci 2003;281(11): 1015–24.

[35] Jones A, Watkins C, White S, Sottos N. Self-healing thermoplastic-toughened epoxy. Polymer 2015;74:254–61.

[36] Karger-Kocsis J. Self-healing properties of epoxy resins with poly (ε-caprolactone) healing agent. Polym Bull 2016;73(11):3081–93.

[37] Yao Y, Wang J, Lu H, Xu B, Fu Y, Liu Y, et al. Thermosetting epoxy resin/ thermoplastic system with combined shape memory and self-healing properties. Smart Mater Struct 2016;25(1):015021.

[38] Szebényi G, Magyar B, Czigany T. Achieving Pseudo-Ductile Behavior of Carbon Fiber Reinforced Polymer Composites via Interfacial Engineering. Adv Eng Mater 2020;23(2):2000822.

[39] Badri W, Miladi K, Nazari QA, Fessi H, Elaissari A. Effect of process and formulation parameters on polycaprolactone nanoparticles prepared by solvent displacement. Colloids Surf A Physicochem Eng Asp 2017;516:238–44.

[40] Yang J, Park SB, Yoon HG, Huh YM, Haam S. Preparation of poly epsilon-caprolactone nanoparticles containing magnetite for magnetic drug carrier. Int J Pharm 2006;324(2):185–90.

[41] Losso J, Khachatryan A, Ogawa M, Godber J, Shih F. Random centroid optimization of phosphatidylglycerol stabilized lutein-enriched oil-in-water emulsions at acidic pH. Food Chem 2005;92(4):737–44.

[42] Karger-Kocsis J, Mahmood H, Pegoretti A. Recent advances in fiber/matrix interphase engineering for polymer composites. Prog Mater Sci 2015;73:1–43.

[43] Mahmood H, Tripathi M, Pugno N, Pegoretti A. Enhancement of interfacial adhesion in glass fiber/epoxy composites by electrophoretic deposition of graphene oxide on glass fibers. Compos Sci Technol 2016;126:149–57.

[44] Dorigato A, Morandi S, Pegoretti A. Effect of nanoclay addition on the fiber/matrix adhesion in epoxy/glass composites. J Compos Mater 2011;46(12):1439–51.

[45] Gaur U, Miller B. Microbond Method for Determination of the Shear Strength of a Fiber/Resin Interface: Evaluation of Experimental Parameters. Compos Sci Technol 1989;34:35–51.

[46] Jones AR, Blaiszik BJ, White SR, Sottos NR. Full recovery of fiber/matrix interfacial bond strength using a microencapsulated solvent-based healing system. Compos Sci Technol 2013;79:1–7.

[47] Invernizzi M, Turri S, Levi M, Suriano R. 4D printed thermally activated self-healing and shape memory polycaprolactone-based polymers. Eur Polym J 2018; 101:169–76.

[48] Wei H, Yao Y, Liu Y, Leng J. A dual-functional polymeric system combining shape memory with self-healing properties. Compos B Eng 2015;83:7–13.